

Interface enhanced precessional damping in spintronic multilayers: A perspective

Cite as: J. Appl. Phys. **131**, 170902 (2022); <https://doi.org/10.1063/5.0080267>

Submitted: 30 November 2021 • Accepted: 14 April 2022 • Published Online: 02 May 2022

 C. Swindells and  D. Atkinson



View Online



Export Citation



CrossMark

Lock-in Amplifiers
up to 600 MHz



Zurich
Instruments



Interface enhanced precessional damping in spintronic multilayers: A perspective

Cite as: J. Appl. Phys. **131**, 170902 (2022); doi: [10.1063/5.0080267](https://doi.org/10.1063/5.0080267)

Submitted: 30 November 2021 · Accepted: 14 April 2022 ·

Published Online: 2 May 2022



C. Swindells¹ and D. Atkinson^{2,a)}

AFFILIATIONS

¹Department of Materials Science and Engineering, University of Sheffield, Sheffield S1 3JD, United Kingdom

²Department of Physics, Durham University, South Road, Durham DH1 3LE, United Kingdom

^{a)}Author to whom correspondence should be addressed: del.atkinson@durham.ac.uk

ABSTRACT

In the past two decades, there have been huge developments in the understanding of damping in multilayered thin films and, more generally, in spin-transport in spintronic systems. In multilayered ferromagnetic (FM)/non-magnetic (NM) thin-film systems, observations of ferromagnetic resonant precession show a strong increase in the fundamental damping when the FM thin films are layered with heavy metals, such as Pt. These observations led to significant theoretical developments, dominated by the “spin-pumping” formalism, which describes the enhancement of damping in terms of the propagation or “pumping” of spin-current across the interface from the precessing magnetization into the heavy metal. This paper presents a perspective that introduces the key early experimental damping results in FM/NM systems and outlines the theoretical models developed to explain the enhanced damping observed in these systems. This is followed by a wider discussion of a range of experimental results in the context of the theoretical models, highlighting agreement between the theory and experiment, and more recent observations that have required further theoretical consideration, in particular, with respect to the role of the interfaces and proximity-induced magnetism in the heavy metal layer. The Perspective concludes with an outline discussion of spin-pumping in the broader context of spin-transport.

© 2022 Author(s). All article content, except where otherwise noted, is licensed under a Creative Commons Attribution (CC BY) license (<http://creativecommons.org/licenses/by/4.0/>). <https://doi.org/10.1063/5.0080267>

I. INTRODUCTION

The magnetization state or domain structure of ferro- and ferri-magnetic materials is determined by the combination of magnetic energies within the system. Any changes to the magnetization state via coherent or incoherent magnetization rotation or domain wall processes are ultimately governed by the damped precessional motion of the constituent magnetic dipoles within the system. This resonant precession and the damping processes that transfer energy from the precessing moments to the lattice are, therefore, fundamentally important in magnetic materials and ultimately constrain the functional magnetic response.

In many applications of bulk magnetic materials, such as those involving quasi-dc changes, precession and damping can be ignored and simpler models are used to represent the processes of magnetization change. In others, precession and damping are fundamental to the material response and must, therefore, be understood and controlled to optimize the performance. For increasingly high frequency applications, the response of bulk metallic ferromagnets is severely

limited by the induction of eddy currents well below the frequencies at which precessional processes and precessional damping losses play a major role. At high frequencies, insulating ferrite and iron-garnet oxide ferrimagnets are, therefore, widely used for applications up to microwave frequencies. In these applications, resonant precession and damping determine the frequency in the GHz regime and the width or quality, Q-factor, of the resonant peak, respectively.

For nanoscale structures and magnetic films with thicknesses of the order of nanometers, eddy current effects may be neglected and precession and damping are critical in determining the functional performance. For field-driven coherent magnetization switching in single domain structures, the reversal time is determined by the damping when the duration of the applied field is long compared to the precessional period, while the precession, rather than damping, controls switching in ultrashort duration magnetic fields.¹ In the case of field-driven domain wall switching, precession and damping determine the wall mobility and an upper field limit and a maximum velocity for free flowing wall motion.²

This limiting “Walker breakdown field” marks the onset of a temporally varying domain wall structure and periodic retrograde wall motion, which present challenges for the functionality of domain wall nanowire device concepts^{3,4} that has been addressed by additional structuring of nanowires.^{5,6} In magnetic thin-films and nanostructured systems in which current flows, magnetization oscillations or switching can be driven by spin transfer torque resulting from spin-polarized current, the dynamics of which also depend on the damping, both for coherent rotation and domain wall processes.

The origin of damping is associated with spin-orbit coupling, for which the theoretical basis is established. For the analysis of ferromagnetic resonance, the separation of the so-called *intrinsic* and *extrinsic* components of the damping is important as it, respectively, allows the attribution of fundamental and defect-induced contributions to the observed linewidth of the ferromagnetic resonance. The intrinsic damping represents the key underlying value of the damping in a perfect system and is determined from the transfer of energy from the fundamental, $k = 0$, precessional magnetization mode to the lattice. Contributions related to other factors including artifacts in the measurement⁷ and higher order precessional modes enabled by defects may be called extrinsic as they relate to additional contributions to the damping that may be removed to determine the fundamental damping of the system. The damping of the higher order modes occurs via the same spin-orbit mechanisms as for the fundamental mode.

It has been two decades since key experimental results showed systematically that intrinsic damping in ultra-thin magnetic (FM) films can be significantly enhanced by layering with selected non-magnetic (NM) metals. Alongside the continuing experimental exploration of this damping enhancement, theoretical developments have created a framework to explain the physical basis for this enhancement, which invokes the propagation of spin current generated at the interface between the FM and NM layers. Interfacial spin transport is a topic of major significance in spintronics and interface enhanced damping contributes to our understanding of spin transport phenomena, including the spin-diffusion length, spin scattering mechanisms, and the role of interfacial factors in spintronic multilayers.

This Perspective presents an accessible description of the key observations and the current understanding of the physical basis for the enhancement of damping in ferromagnetic thin-films layered with non-magnetic materials. This work is not intended as a comprehensive review but aims to provide a synthesis of experimental reports and theoretical descriptions.

The paper is sub-divided with Sec. II describing the early experimental observations of damping in FM/NM multilayers to set the scene, followed in Sec. III with a description of the theoretical basis for the damping enhancement, which includes an introduction to ferromagnetic resonance and damping and an outline of the physics of damping in ferromagnets and in FM/NM systems. Section IV discusses significant experimental results in the context of the theoretical framework described in Sec. III, providing a basis for understanding what can be explained and what issues remain of some debate. Section V broadens the Perspective to related developments of understanding in spin transport, and Sec. VI summarizes and concludes the current status.

II. EARLY OBSERVATIONS OF INTERFACE ENHANCED DAMPING IN THIN-FILM SYSTEMS

A series of results from studies of damping in multilayered FM/NM thin-film systems in the early 2000s highlight and demonstrate the key observations. Prior to this, critical works on FM thin films interfaced with NM substrates indicated diffuse electronic transmission across the interface from the FM layer during ferromagnetic resonance in Fe, Ni, and $\text{Ni}_{80}\text{Fe}_{20}$ ⁸ and increased damping in ultrathin Fe layers deposited on Ag and capped with Au with decreasing FM layer thickness.⁹

The first significant results from 2001 were obtained from a systematic study of ferromagnetic damping as a function of the FM thickness in ultrathin Permalloy ($\text{Ni}_{80}\text{Fe}_{20}$) films deposited with 5 nm thick under and over layers of various non-magnetic transition metals was reported by Mizukami *et al.* in 2001,^{10,11} see Fig. 1(a). This showed a large increase in the damping for the FM layered with Pd or Pt and a smaller or no increase for Ta and Cu, respectively. Critically, the enhancement of the damping was strongly and non-linearly dependent upon the ferromagnetic thickness.

A contemporary study¹² of ultrathin Fe layers separated by 40 monolayers of Au showed a FM thickness (t) dependence of the damping enhancement that scaled linearly with $1/t$, suggesting an interfacial basis for the enhanced damping.

The enhancement of the damping is also dependent on the NM layer thickness, which is characterized by an increase in the damping that rises rapidly within the first 1 nm and tends to a plateau at greater thicknesses,¹³ see Fig. 1(b). Early work also showed that the insertion of a Cu spacer layer of increasing thickness between the FM layer and a high damping NM metal, such as Pt, rapidly reduced the damping toward to the original uncapped FM level with a few 10s nanometers of Cu, see Fig. 1(c).

Finally, a critical early report by Saitoh *et al.*¹⁴ demonstrated in a $\text{Ni}_{81}\text{Fe}_{19}/\text{Pt}$ system that an electromotive force, *emf*, and associated charge current are generated orthogonal to the film thickness at ferromagnetic resonance, as shown in Fig. 2.

III. PHYSICAL BASIS OF ENHANCED DAMPING IN FM/NM SYSTEMS

The observations of enhanced damping in FM/NM systems drove efforts to explain the physical basis of this phenomenon. The early experimental works of Heinrich *et al.*⁹ and Mizukami *et al.*¹¹ suggested an enhanced role for the spin-orbit coupling (SOC) at the interface, while Urban *et al.*¹² explained the additional damping in terms of the flow of spin angular momentum generated by precession in one FM layer through the NM layer to a second FM layer where it relaxes, as proposed by Berger.^{15,16} The notion of additional damping enabled by a precession driven spin current across the FM/NM interface that dissipated within the NM layer was taken up by Mizukami *et al.*,¹³ while the critical theoretical description of this mechanism for enhanced damping, now commonly termed “spin pumping,” was developed in a series of key papers by Tserkovnyak *et al.*^{17–19}

The enhancement of the damping in FM/NM systems has been theoretically described most commonly by the spin-pumping

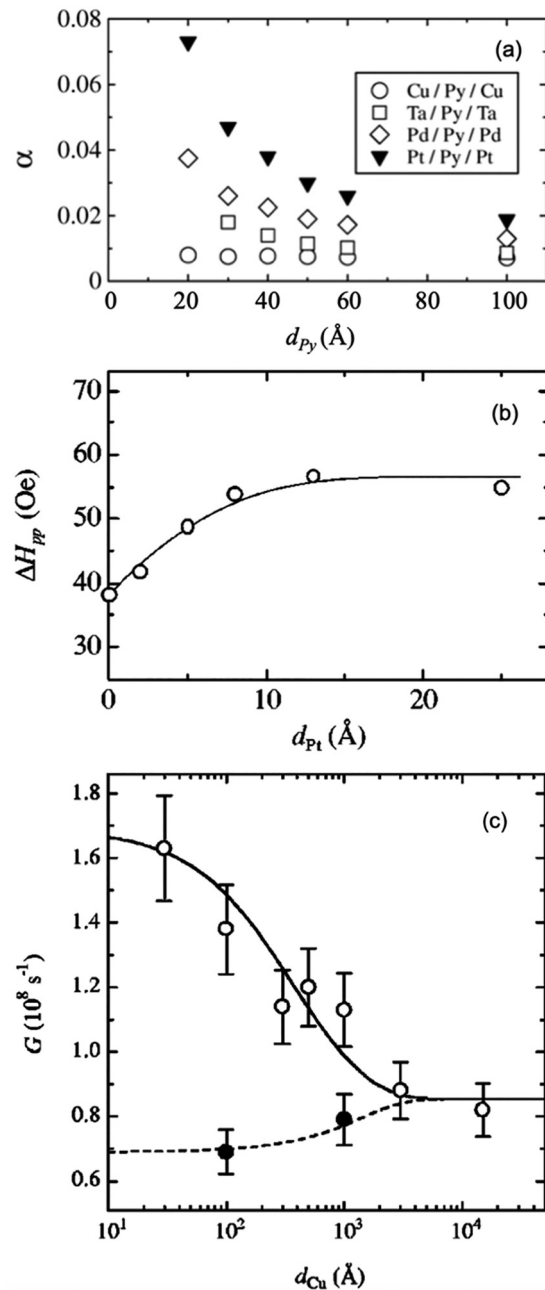


FIG. 1. (a) The variation of the Gilbert damping parameter in NM/FM/NM systems as a function of $\text{Ni}_{80}\text{Fe}_{20}$ film thickness (d_{Py}) for different NM metals. Reproduced with permission from Mizukami *et al.*, Jpn. J. Appl. Phys. **40**, 580 (2001). Copyright 2001 The Japan Society of Applied Physics. (b) The influence of the Pt layer thickness, d_{Pt} , on the linewidth of the ferromagnetic resonance in Pt/ $\text{Ni}_{80}\text{Fe}_{20}$ /Pt damping, and (c) the effect of the thickness of a non-magnetic Cu spacer layer, d_{Cu} , between $\text{Ni}_{80}\text{Fe}_{20}$ and Pt (open symbols) on the effective Gilbert damping coefficient compared to Cu/ $\text{Ni}_{80}\text{Fe}_{20}$ /Cu (solid symbols) reference samples. Reproduced with permission from Mizukami *et al.*, Phys. Rev. B **66**, 104413 (2002). Copyright 2002 the American Physical Society.

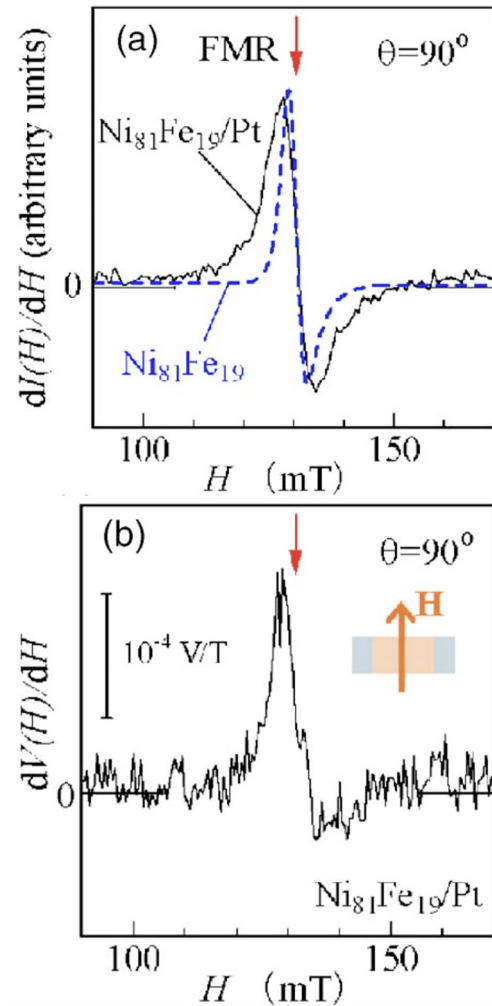


FIG. 2. (a) Ferromagnetic resonance in $\text{Ni}_{80}\text{Fe}_{20}$ and $\text{Ni}_{81}\text{Fe}_{19}/\text{Pt}$ bilayers, showing larger damping with Pt. (b) Shows a voltage measured orthogonal to the film thickness that is coincident with the ferromagnetic resonance and associated with the flow of spin current from the $\text{Ni}_{80}\text{Fe}_{20}$ into Pt as a result of precession. Reproduced with the permission from Saitoh *et al.*, Appl. Phys. Lett. **88**, 182509 (2006). Copyright 2006 AIP Publishing LLC.

model in which spin angular momentum is transferred across an interface and then relaxes in the NM material, while other theoretical developments have focused on the s - d and d - d exchange across the interface²⁰ and a tight-binding electronic model that includes SOC was developed by Barati *et al.*²¹ Before discussing these theoretical approaches to damping in FM/NM systems in more detail, it is useful to first outline the common description of precession and damping via the Landau–Lifshitz–Gilbert formalism and to summarize the physical basis for damping within ferromagnetic materials and the mechanisms of spin-dependent scattering.

A. Landau-Lifshitz-Gilbert formalism

Dynamic magnetization can be described within a framework proposed by Landau and Lifshitz²² in which the precessional motion of a magnetization, \vec{M} , about an effective magnetic field, \vec{H}_{eff} , as illustrated in Fig. 3(a), is described by

$$\frac{d\vec{M}}{dt} = -\gamma\mu_0(\vec{M} \times \vec{H}_{\text{eff}}) \quad (\text{SI}), \quad (1)$$

$$\frac{d\vec{M}}{dt} = -\gamma(\vec{M} \times \vec{H}_{\text{eff}}) \quad (\text{CGS}), \quad (2)$$

where γ is the gyromagnetic ratio that scales the total spin-orbit angular momentum to the magnetic moment and μ_0 is the permeability of free space. Without energy loss, the magnetization would precess continuously. However, in real systems, energy is dissipated and the amplitude of precession decreases until the magnetization aligns with the effective field, as shown in Fig. 3(b). Landau and Lifshitz (LL) represented this with the addition of a damping term,

$$\frac{d\vec{M}}{dt} = -\gamma\mu_0(\vec{M} \times \vec{H}_{\text{eff}}) - \frac{\lambda\mu_0}{M_s^2}\vec{M} \times (\vec{M} \times \vec{H}_{\text{eff}}) \quad (\text{SI}), \quad (3)$$

$$\frac{d\vec{M}}{dt} = -\gamma(\vec{M} \times \vec{H}_{\text{eff}}) - \frac{\lambda}{M_s^2}\vec{M} \times (\vec{M} \times \vec{H}_{\text{eff}}) \quad (\text{CGS}), \quad (4)$$

where λ is a damping frequency, the inverse of the relaxation time, τ_m . For heavily damped systems, this equation results in fast relaxation. Gilbert²³ modified the LL equation, introducing a dimensionless damping parameter, resulting in what is now called the

Landau-Lifshitz-Gilbert or LLG equation,

$$\frac{d\vec{M}}{dt} = -\gamma\mu_0(\vec{M} \times \vec{H}_{\text{eff}}) + \frac{\alpha}{M_s} \left(\vec{M} \times \frac{d\vec{M}}{dt} \right) \quad (\text{SI}), \quad (5)$$

$$\frac{d\vec{M}}{dt} = -\gamma(\vec{M} \times \vec{H}_{\text{eff}}) + \frac{\alpha}{M_s} \left(\vec{M} \times \frac{d\vec{M}}{dt} \right) \quad (\text{CGS}), \quad (6)$$

where α is the dimensionless Gilbert damping parameter, which reflects the fundamental damping of the system. In practice, there is an equivalence between the LL and LLG equations, as the damping is sufficiently small in real materials. Large values of damping result in faster relaxation of the magnetization toward the effective magnetic field direction.

For a given magnetic material at ferromagnetic resonance, a solution for the resonance condition that satisfies the LLG formula is known as the Kittel equation,^{24,25} for thin-films the resonant frequency, f , is related to the effective field within the system arising from any externally applied magnetic field, H_{ext} , magnetic anisotropy, H_a , and the effective magnetization, M_{eff} , of the system

$$f = \frac{\gamma\mu_0}{2\pi} \sqrt{(H_{\text{ext}} + H_a)(H_{\text{ext}} + H_a + M_{\text{eff}})} \quad (\text{SI}), \quad (7)$$

$$f = \frac{\gamma}{2\pi} \sqrt{(H_{\text{ext}} + H_a)(H_{\text{ext}} + H_a + 4\pi M_{\text{eff}})} \quad (\text{CGS}). \quad (8)$$

The resonant response of a magnetic material forms a Lorentzian line shape in the magnetic field or frequency, the line-width of which is dependent upon the total system damping. In the frequency domain, the full-width half-maximum (FWHM) line-width, Δf , is derived as²⁵

$$\Delta f = \frac{\gamma\mu_0}{2\pi} \alpha (2H_{\text{ext}} + 2H_a + M_{\text{eff}}) \quad (\text{SI}), \quad (9)$$

$$\Delta f = \frac{\gamma}{2\pi} \alpha (2H_{\text{ext}} + 2H_a + 4\pi M_{\text{eff}}) \quad (\text{CGS}). \quad (10)$$

The subsequent analysis follows in CGS magnetic units. In the magnetic field domain, the homogeneous linewidth is represented by the FWHM of the resonance as^{25,26}

$$\Delta H = \frac{4\pi\alpha}{\gamma} f. \quad (11)$$

While the LLG equation is widely used to model dynamic behavior of magnetic moments, it is not without several assumptions that do not necessarily hold, particularly, within itinerant systems.²⁷ The dynamic behavior of the spins is treated as a uniform precession, the $k = 0$ mode, which is not the case at high temperatures, where additional excited modes can enhance the scattering²⁸ and, therefore, the damping of a system.²⁹ At finite temperatures, the LLG equation can be modified with the inclusion of a thermal noise term to account for temperature effects,³⁰ with the magnetization

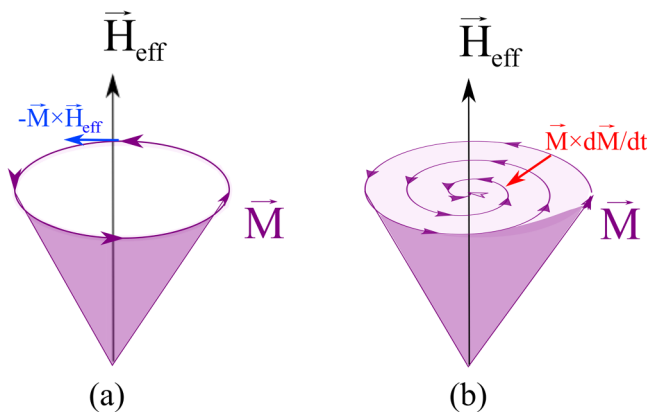


FIG. 3. Illustration of (a) the precession of a magnetic moment about an effective magnetic field and (b) damping acting perpendicular to the direction of the precessional motion, causing the magnetization to align with the magnetic field.

vector considered of fixed magnitude and unchanged with temperature.

Importantly, measurement artifacts and imperfections in the magnetic material can additionally broaden the resonance linewidth. In the FMR measurement, the so-called radiative damping, linked to magnetic interactions with the measurement circuit, increases the linewidth, which is particularly relevant for the analysis of ultra-low damping systems. Imperfections within the magnetic material may be structural point or line defects or associated with local variations due to impurities or compositional changes. These defects act to disrupt the global uniform precessional mode, causing local variations of the precession that broaden the resonance peak and increase the total damping. This enhancement is termed inhomogeneous line broadening and may be considered to represent the extrinsic contributions to the damping. In the LLG formalism, this adds an extra term to the field linewidth³¹

$$\Delta H = \frac{4\pi\alpha}{\gamma}f + \Delta H_0, \quad (12)$$

with ΔH_0 representing the additional damping contributions. In FMR experiments, typically, either the frequency or the external magnetic field is fixed, and the other parameter varied, producing either of these linewidths, though it is possible to convert between field and frequency domains,³² and, critically, it is possible to separate the intrinsic and extrinsic contributions to the damping.

B. The physical basis of damping in transition metal ferromagnets

Damping requires the transfer of energy and angular momentum from the precessing magnetic moments to the lattice. For itinerant ferromagnets, relevant to the magnetic transition metals and their alloys, damping has been effectively described by the formation and re-combination of transitory, i.e., short-lived, electronic states. Spin-orbit coupling is critical to this process and depends on the electronic structure around the Fermi level.^{33–35} Kambersky's torque correlation model has provided the basis for the most successful quantitative analysis of damping in Fe, Co, and Ni.^{35,36} The process involves the annihilation of uniform-mode magnons, associated with the precessing magnetization, where precession causes angular variations of the electronic spin orientation. The coupling of this angular spin variation with the lattice via the spin-orbit interaction effects a torque that modifies the electronic states around the Fermi level creating electron-hole pairs, and it is the re-combination of these pairs that releases energy that is dissipated to the lattice. The electron-hole pairs can be generated within the same energy band, the so-called intraband excitations, or between bands, creating interband pairs. The temperature dependence of the damping can be used to distinguish between these modes, the details of which are summarized elsewhere.³⁷

C. Spin-dependent scattering and the spin-diffusion length

Before discussing theories of damping enhancement in FM/NM systems and because spin transport is invoked to explain such phenomena, it is helpful to introduce the processes of spin

relaxation and the length-scales over which they occur. Unlike ferromagnetic transition metal species, which have spin-split d bands at the Fermi energy, in bulk non-ferromagnetic metals, the spin states are equal at the Fermi energy, so net scattering is spin independent. When a spin-polarized current passes into such a metal, spin-flip scattering events reduce the net spin polarization of the current until it becomes unpolarized.

Two mechanisms are commonly considered for the processes of spin-relaxation in metals, both depend upon the spin-relaxation time, τ_{sf} , and the electron momentum scattering time, τ_e . For the so-called *Elliot-Yafet* (EY) scattering,^{38,39} each momentum scattering event presents an opportunity for a spin-flip to occur, the probability of which depends on the strength of the SOC. The spin-flip scattering relaxation time is, therefore, proportional to the rate of momentum scattering, i.e., $\tau_{sf} \propto \tau_e$.⁴⁰

The second mechanism termed *D'yakonov-Perel* (DP) spin relaxation⁴¹ is prevalent in systems with inversion asymmetry, which may be created at interfaces or is present in the bulk in some systems. Spins precess about the effective spin-orbit (SO) field and de-phase as they do so.⁴² The spin-flip relaxation time in this case is inversely proportional to the momentum scattering, $\tau_{sf} \propto 1/\tau_e$. Both mechanisms can occur within a material, however, for common non-ferromagnetic metals such as Pt, the DP contribution is suppressed at room temperatures and the EY scattering dominates.^{42,43}

The length-scale over which the polarization of a spin-current decreases is described by the *spin-diffusion* length, λ_{sd} , and the related, but not identical, *spin-flip* length.⁴⁴ λ_{sd} is defined as the distance over which the spin polarization is reduced by a factor $1/e$. It is related to momentum scattering via⁴²

$$\lambda_{sd} = \sqrt{\frac{v_F l_e \tau_{sf}}{3}}, \quad (13)$$

with Fermi velocity, v_F , and the electron mean free path, $l_e = v_F \tau_e$.¹⁸ An outstanding issue in the literature is the value of λ_{sd} . This is one of the parameters that determines the enhancement of the magnetic damping of a layered system and must be well-defined to quantitatively model the response of the system. However, reported values of λ_{sd} vary by more than an order of magnitude, which may be linked to the measurement method and the assumptions upon which it is derived.⁴⁴

D. Quantum mechanical theory of interface enhanced damping

A description of the enhancement of Gilbert damping with interfaces between FM and NM materials based on tight-binding electronic structure calculations was developed by Barati *et al.*,²¹ following the theoretical approach of Kambersky.⁴⁵ An ideal layer-by-layer atomic structure forms the basis of the tight-binding model of localized orbitals described by a Hamiltonian that includes spin-orbit interactions between the first and second nearest neighbors. Damping was calculated as a perturbation using the Hamiltonian to determine the relaxation arising from inter- and intra-band transitions. Crucially, the calculated damping is

dependent upon an electron scattering rate, the density of states, and the SOC strength.

For FM/NM bilayers with different NM metals, the damping contribution is the largest at the interface for all NM metals studied, with the rate at which the damping contributions for each layer falling to zero, dependent upon the electron scattering rate. For NM metals with a full d band, such as Cu or Ag, the interfacial enhancement is very small, arising from modification of the electronic structure of the upper FM layer due to orbital overlap. For heavy metals, such as Pd and Pt, the d band crosses the Fermi energy, giving a large density of states that provides opportunities for hybridization, and the enhancement of the damping is much greater,²¹ see Fig. 4. In this model, the most significant enhancement of the damping arises from the first monolayer of the NM metal, the enhancement saturates within a few monolayers and is closely associated with a large SOC and a large density of states.

This model shows a reciprocal dependence of the damping on the ferromagnetic layer thickness in the Co/NM systems studied.

E. Spin pumping model of interface enhanced damping

An early model for the enhancement of the resonance linewidth occurring when a non-magnetic material is in contact with a ferromagnet was given by Silsbee *et al.*⁸ They describe a “magnetization current” from the diffusion of exchange-field polarized electrons from the excited ferromagnet into the paramagnet. This was shown to be much larger than the effect of the microwave field alone on the Pauli paramagnetic moment of the NM material.

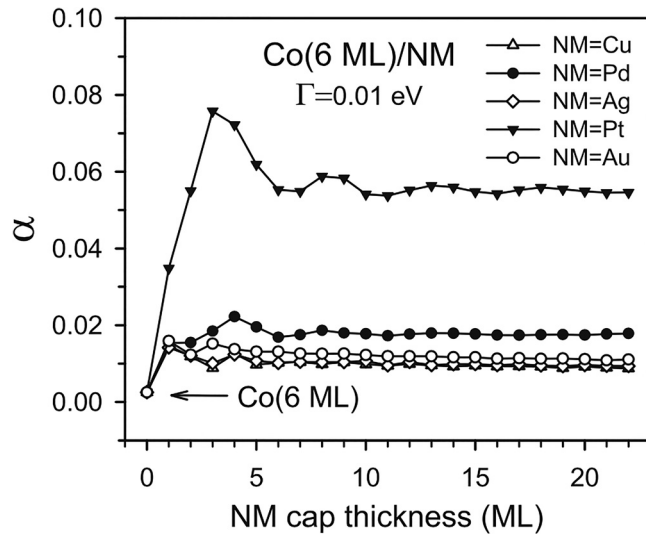


FIG. 4. Gilbert damping constant in a six monolayer fcc Co layer as a function of NM layer thickness for different NM metals, calculated using a tight-binding model with spin-orbit interactions. Reproduced with permission from Barati *et al.*, Phys. Rev. B **90**, 014420 (2014). Copyright 2014 the American Physical Society.

A further development proposed by Berger^{15,46} incorporated spin waves and itinerant conduction electrons at an interface. According to Berger, sharp interfaces enable electrons to cross the momentum gap between spin-up and spin-down Fermi surfaces while emitting or absorbing a magnon of energy $\hbar\omega$. For a precessing ferromagnet, the spins at an interface drive transitions of the conduction electrons between spin-up and spin-down bands, leading to a non-zero difference in the electrochemical potential between spin-up (μ_s^\uparrow) and spin-down (μ_s^\downarrow) levels, resulting in spin being injected across an interface.⁴⁶

The most widely used approach to describe the physical basis for the enhancement of magnetic damping in FM/NM interfaced systems is the commonly termed “spin-pumping” model developed by Tserkovnyak *et al.*^{17–19,47–49} This model builds upon the same physics as the earlier models and utilizes the scattering theory approach developed by Brouwer⁵⁰ (to compute the parametric pumping of charge current in non-magnetic systems) to represent the spin current. The essence of spin-pumping is an enhancement of the damping resulting from the generation, propagation, and absorption of a spin current, \vec{I}_s , in a NM layer, driven by the precessing magnetization in a FM layer. Figure 5 illustrates this process.

The magnitude of the spin current across the FM/NM interface depends on both the NM material parameters and the physical properties of the interface itself. The process is most easily understood when the magnetic layer is an insulator, such as ferromagnetic yttrium iron garnet (YIG), but metallic ferromagnetic layers are also common. The pumping of the spin current generated by the precessing magnetization is characterized in terms of a *spin-mixing conductance*, $G^{\uparrow\downarrow}$, (Ω^{-1}), or more commonly the spin mixing conductance per unit area, A , per conductance channel, $g^{\uparrow\downarrow} = G^{\uparrow\downarrow}/(A e^2/h)$,⁵¹ which itself can be expressed as¹⁹

$$g^{\uparrow\downarrow} = g_r^{\uparrow\downarrow} + i g_i^{\uparrow\downarrow}, \quad (14)$$

where $g_r^{\uparrow\downarrow}$ represents the transmitted part of the spin current aligned with the transverse component of the spin accumulation

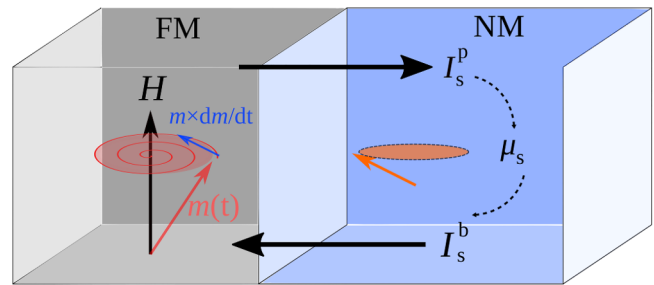


FIG. 5. Simplified schematic illustration of the spin pumping process. A precessing magnetization in the FM layer drives a spin current across the interface, with instantaneous polarization orthogonal to $\vec{m}(t)$ and rate of magnetization change, $d\vec{m}/dt$. For realistic systems, the pumped spin current results in a spin accumulation, which drives a spin current back into the FM layer, with the component of \vec{I}_s^b parallel to \vec{m} transmitted.

and $g_i^{\uparrow\downarrow}$ the de-phasing of the spins due to the precession about the direction of the FM magnetization as they transfer across an interface.⁵² For metallic interfaces, it is commonly assumed, and has been shown from first-principles calculations, that for typical metallic interfaces^{53,54} $g_r^{\uparrow\downarrow} \gg g_i^{\uparrow\downarrow}$ and, therefore,

$$g^{\uparrow\downarrow} \approx g_r^{\uparrow\downarrow} \approx g_N^{SH}, \quad (15)$$

where g_N^{SH} is the Sharvin conductance, which quantifies the number of transport channels per unit area for one spin across the interface between the two materials.¹⁹

For an ideal conductor, the imaginary part of the spin mixing conductance may be neglected such that the instantaneous spin current pumped into the NM is then

$$\vec{I}_S = \frac{\hbar}{4\pi} g_r^{\uparrow\downarrow} \vec{m} \times \frac{d\vec{m}}{dt}, \quad (16)$$

with $\vec{m} = \vec{M}/M_s$, where M_s is the saturation magnetization.¹⁹ As evident in Eq. (16), and illustrated in Fig. 5, the polarization of the pumped spin current is orthogonal to both \vec{m} and $\frac{d\vec{m}}{dt}$; however, a component of the polarization remains aligned with \vec{H} .

The pumped spin current thus contains both ac and dc components. It is the ac component that is key to measurements of spin transport focusing on modulations of the damping through spin pumping, while the dc component is relevant for measurements of spin transport using the inverse spin Hall effect. The dc component is given by the time average of this over precessional cycles,⁵⁵

$$\langle \vec{I}_S^p \rangle = \vec{I}_{DC} = \hbar \omega g_r^{\uparrow\downarrow} \sin^2 \theta / 4\pi, \quad (17)$$

where θ is the precession cone angle and \vec{I}_{DC} is aligned along the equilibrium direction of \vec{m} .

The pumped spin current decays within the NM layer over a characteristic length-scale, λ_{sd} , due to the mechanisms described earlier. For ideal NM spin-sink materials, the spin relaxation is rapid, occurring over short length-scales and resulting in dissipation of the pumped current. However, in diffuse systems, where the spin relaxation is smaller than the rate at which current is pumped, a spin accumulation builds within the NM layer, resulting in an additional current that flows back into the FM layer, \vec{I}_S^B .¹⁸

This process of spin accumulation driving a spin current is analogous to a conventional battery, for which reason, this mechanism for the transfer of spin angular momentum has been termed a spin battery.⁴⁷ In the general case, the spin current, \vec{I}_S , has two components

$$\vec{I}_S = \vec{I}_S^p + \vec{I}_S^B, \quad (18)$$

where \vec{I}_S^p represents the spin current pumped into the NM layer. Considering the back flow current, \vec{I}_S^B , there is a proportion of the backflow current that is parallel to the instantaneous magnetization, which is nullified by the opposite flow of spin current from the FM, while the remaining component is perpendicular to the magnetization is \vec{I}_S^B .¹⁹ The back flow of spin current may be neglected

for ideal NM spin-sink materials but will limit the net spin current and the resulting enhancement of the damping when there is significant spin accumulation, where the NM needs to be considered a diffuse conductor.

For real conductors, diffusive spin transport and spin accumulation, $\vec{\mu}_s$, are needed to determine \vec{I}_S accounting for the back flowing spin current \vec{I}_S^B that is orthogonal to the magnetization, where the resulting spin current is

$$\vec{I}_S = \frac{\hbar}{4\pi} g_r^{\uparrow\downarrow} \vec{m} \times \frac{d\vec{m}}{dt} - \frac{g_r^{\uparrow\downarrow}}{4\pi} \vec{m} \times \vec{\mu}_s \times \vec{m}, \quad (19)$$

in which it is noted that $\vec{\mu}_s$ is aligned with $\vec{m} \times \frac{d\vec{m}}{dt}$.

In a FM/NM system, the propagation of the net spin current \vec{I}_S into the NM layer increases the damping because spin angular momentum is transferred out of the FM and absorbed in the NM layer. With the conservation of angular momentum and because the spin current is polarized orthogonal to the magnetization, this results in an additional effective damping torque on the magnetization.¹⁹ The magnetization dynamics of a FM/NM system can, therefore, be modeled phenomenologically by incorporating this additional torque into the LLG equation that was introduced earlier, so the dynamic magnetization can be represented by

$$\frac{d\vec{m}}{dt} = -\gamma(\vec{m} \times \vec{H}_{\text{eff}}) + \alpha_0 \vec{m} \times \frac{d\vec{m}}{dt} + \frac{\hbar\gamma}{4\pi M_s} \vec{m} \times \vec{I}_S \times \vec{m}, \quad (20)$$

where α_0 represents the damping in the uncapped FM layer. Introducing the expression for the spin current in an ideal spin sink, from Eq. (16), the modified LLG equation becomes

$$\frac{d\vec{m}}{dt} = -\gamma(\vec{m} \times \vec{H}_{\text{eff}}) + \left(\alpha_0 + \frac{\hbar\gamma}{4\pi M_s} g_r^{\uparrow\downarrow} \right) \vec{m} \times \frac{d\vec{m}}{dt}, \quad (21)$$

from which it is apparent, from the second term in brackets, that the ferromagnetic damping increases beyond that obtained in the uncapped FM layer.

In summary, “precession-pumped” spin current relaxes within the NM layer, enhancing the intrinsic magnetic damping by effectively providing an additional pathway for energy loss for the uniform mode precession to decay.

IV. ANALYSIS OF EXPERIMENTAL OBSERVATIONS IN RELATION TO THEORETICAL MODELS

A. Dependence on the thickness of FM layer

The enhancement of damping due to interfacial effects is commonly modeled as the addition of a NM interface related term, α_s , to the bulk-like FM Gilbert damping, α_0 , to give a total damping $\alpha = \alpha_0 + \alpha_s$. Tserkovnyak *et al.*¹⁷ applied their spin pumping model to estimate the damping enhancement observed in the early data of Mizukami *et al.*¹¹ for $\text{Ni}_{80}\text{Fe}_{20}$ sandwiched between different NM metals. The model, in general, is in good agreement with the data, reflecting the reciprocal dependence of the enhancement on the FM thickness and matching the magnitude of the damping enhancement, see Fig. 6.

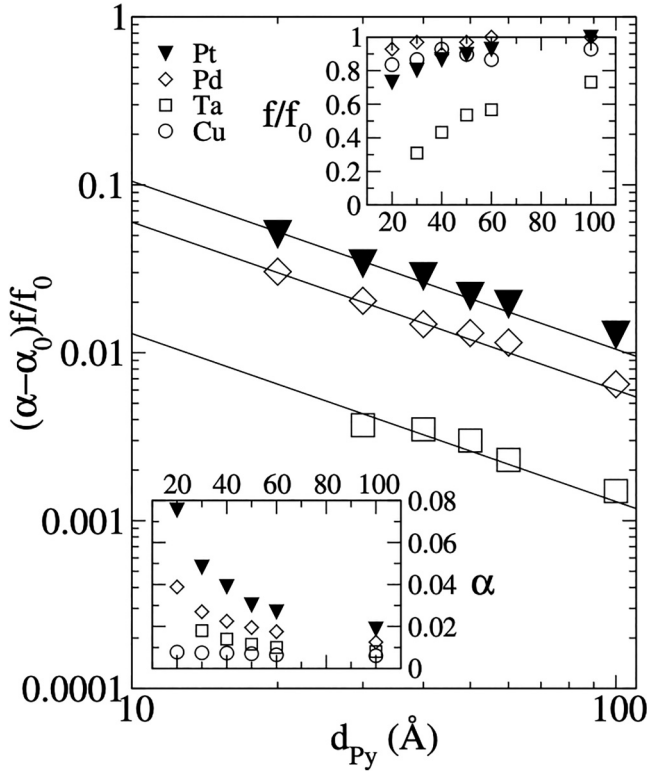


FIG. 6. Comparison of experimental data and early spin pumping model for the enhancement of damping in NM/Ni₈₀Fe₂₀/NM thin-film systems. Reproduced with permission from Tserkovnyak *et al.*, Phys. Rev. Lett. **88**, 117601 (2002). Copyright 2002 the American Physical Society.

B. The NM layer and spin mixing conductance

In the spin-pumping model, the enhancement of the damping, α_s , is a function of the NM layer properties that can be expressed as¹⁸

$$\frac{\alpha_s}{\alpha_s^\infty} = \frac{1}{1 + [\sqrt{\epsilon} \tanh(L/\lambda_{sd})]^{-1}}, \quad (22)$$

where L is the NM layer thickness and ϵ represents the ratio of the momentum scattering time (or length) to the spin-flip scattering time (or length) in the EY formalism discussed earlier. The value of ϵ depends upon the strength of the SOC in the NM material, which depends strongly on the atomic number, with larger values producing shorter spin-diffusion lengths and higher damping. Which is a key reason why Pt has a much shorter spin-diffusion length compared to Cu⁴⁴ and why heavy metals, such as Pt, are referred to as good *spin-sinks*, as the spin current dissipates over a short length-scale in the layer. α_s^∞ is the enhancement of the damping assuming a perfect spin sink with infinite spin-flip rate in the NM layer, i.e., no backflow current. It is to be noted that the spin-diffusion length obtained from spin-pumping analysis of

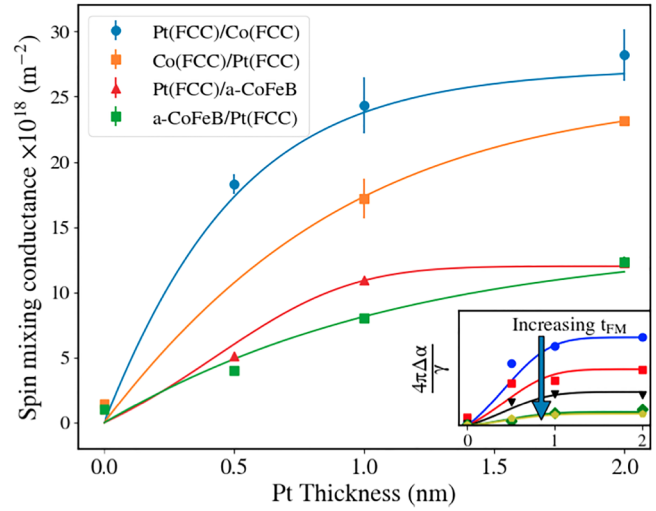


FIG. 7. Examples of the variation of the spin mixing conductance as a function of Pt thickness, determined for ferromagnetic materials of thickness from 2 to 15 nm and different ordering of the NM and FM layer growth. The inset shows the variation of the effective damping for different FM thicknesses (2, 3, 5, 10, and 15 nm following the arrow) of the Pt/CoFeB system as a function of Pt thickness. Reproduced with permission from Swindells *et al.*, Phys. Rev. B **99**, 064406 (2019). Copyright 2019 the American Physical Society.

damping typically produces low values compared to other methods.⁵⁶

The enhancement of the damping also depends on the ferromagnetic layer thickness t ,⁵⁷

$$\alpha_s = \frac{\gamma \hbar}{4\pi M_s t} g_{\text{eff}}^{\uparrow\downarrow}, \quad (23)$$

where $g_{\text{eff}}^{\uparrow\downarrow}$ is the effective spin-mixing conductance per unit area for a single NM layer thickness. This effective spin-mixing conductance is the parameter typically measured in FMR experiments and accounts for changes in the sample quality, given as^{18,58}

$$g_{\text{eff}}^{\uparrow\downarrow} = \frac{g^{\uparrow\downarrow}}{1 + g^{\uparrow\downarrow} \left(\frac{\hbar \sigma}{e^2 \lambda_{sd}} \tanh\left(\frac{t}{\lambda_{sd}}\right) \right)^{-1}}, \quad (24)$$

with $g^{\uparrow\downarrow}$ being the intrinsic spin-mixing conductance of the FM/NM interface and σ , t , and λ_{sd} being the conductivity, thickness, and spin-diffusion length of the NM layer. It should be noted this assumption holds in the case assuming minimal two-magnon scattering.⁵⁹

In the spin-pumping formalism, the key parameters are, therefore, ϵ , λ_{sd} , and $g^{\uparrow\downarrow}$ and there is a dependence on both the thickness of the FM and the NM layers, so a full experimental analysis should involve both the thickness dependence of the FM and the NM layers, see, for example, Fig. 7. In this figure, spin-pumping analysis was undertaken simultaneously fitting the NM and FM thickness dependencies of the data.⁵⁶ This showed different

spin-flip probabilities and spin-mixing conductances associated with different FM/NM interface structures, and that the inclusion of a thickness-dependent spin-diffusion length gave values for the spin-diffusion length for Pt that are comparable with the larger values obtained by other methods, such as via spin Hall angle determination.⁵⁶

In the tight binding analysis, the damping contribution, arising from the SOC of the heavy metal at the interface, decays in a roughly exponential way with increasing NM thickness.²¹ However, while in the spin-pumping the decay length-scale is associated with the spin-diffusion length, the characteristic decay length in the tight binding model, which is also relatively short, cannot be directly linked to the spin-diffusion length. The experimental data from Azzawi *et al.*⁶⁰ shows a NM thickness dependence that follows a comparable short length-scale trend to that calculated in the tight binding approximation, see Fig. 8.

C. The FM/NM interface and spin memory loss

In addition to the thickness dependence of the FM and NM layers, the interfaces between these layers also play a significant role in the enhancement of the damping and spin transport in these systems. Studies of damping in FM/NM systems where the interface was increasingly intermixed by ion-beam irradiation have shown increasing disorder at the interface and an associated increase in

the extrinsic contribution to the damping.^{61,62} It has also been shown that the initial growth of a HM layer on a FM leads first to an increase of the extrinsic contribution to the total damping. This is linked to non-uniform coverage of the HM on the FM layer, creating localized variations at the interface that generate the additional magnon modes.⁶⁰ With thicker more uniform HM coverage, the extrinsic contribution was reduced, but the intrinsic damping remains enhanced, see Fig. 8(a).

Theoretically, the FM/NM interface is critical to the enhancement of damping both in the tight bonding model and for spin-pumping. The arrangement of the atoms across the interface determines the local electronic structure and the resultant $d-d$ hybridization and local enhancement of SOC of the FM at the interface, which are shown to enhance the intrinsic damping in the tight binding model for very thin HM layers, see Fig. 8(b). In the spin-pumping formalism, the interfacial electronic structure determines the conduction channels and, hence, the transparency of the interface for spin current propagation. In this model, better matching of the conduction channels across the FM/NM interface should increase the conductance and reduce any back flow of spin current, thus increasing $g^{\uparrow\downarrow}$ and the overall damping, assuming the NM is a good spin-sink.

Observations of damping in metallic FM/NM systems, where different local structures at the interface were created, show that the damping enhancement is associated with the local structure and that matching of the crystal structure across the interface enhances the damping and the effective $g^{\uparrow\downarrow}$ in spin pumping analysis.^{56,60,63} For spin-pumping in insulator/normal metal bilayers, this has recently been explained theoretically in terms of crystal field effects.⁶⁴

The loss of spin polarization of the current in 3d metal/Pt and 3d metal/Pd systems in magnetoresistance measurements has long been attributed to an interfacial contribution termed *spin memory loss*,⁶⁵ due to diffusion and disorder at the interface. Rojas-Sanchez *et al.*,⁶⁶ reported the role of this contribution with respect to damping experiments and spin pumping analysis, where the spin flipping term, δ , is defined as the ratio between the effective interface thickness and the interface spin-diffusion length, which becomes short with the disorder. This term was reported to account for enhanced interfacial depolarization of the spin current injected into Pt.

An adaption to the model by Chen and Zhang⁶⁷ was proposed to account for some of these additional terms by the explicit inclusion of interfacial spin-orbit coupling into the spin pumping framework. Enhanced SOC at the interface between a FM and heavy metal was shown theoretically to give increased spin current absorption at the interface. Furthermore, this model was able to account for increased interfacial disorder through the modulation of the exchange parameter via the local variation of the saturation magnetization, which affects the magnitude of the pumped spin current and, hence, the damping. Since both alloy composition and interface disorder affect the magnetization, the model is able to account for these effects, which were not captured in the spin mixing conductance of the original model.

It is thus clear that in FM/NM systems, it may be asserted that the interface between the layers plays a key role in the enhancement of the damping and that both the interface structure and the SOC

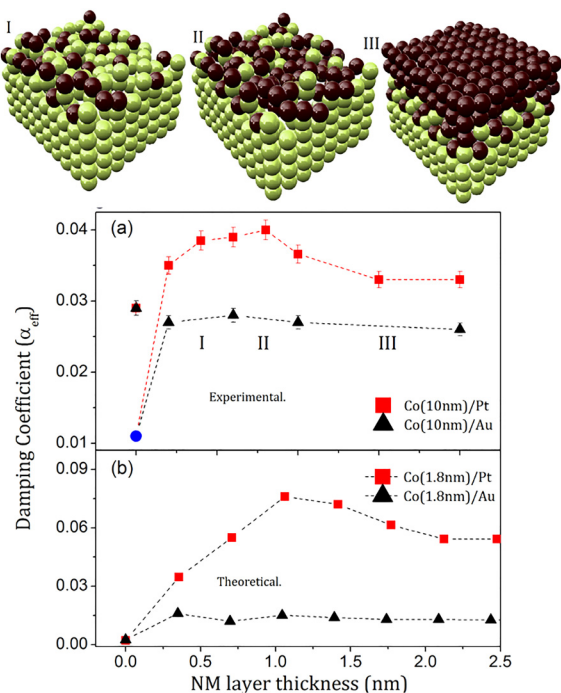


FIG. 8. Comparison of ultrathin NM thickness dependence of damping from experimental measurements and tight binding model for Co capped with Au or Pt. Reproduced with permission from Azzawi *et al.*, Phys. Rev. B **93**, 054402 (2016). Copyright 2016 the American Physical Society.

at the interface contribute. Furthermore, it is also apparent that spin-flip scattering of the spin current should consider additional contributions specifically associated with the interfaces in addition to scattering within the bulk NM layer.

D. Proximity-induced magnetization, damping, and spin transport

NM metals and particularly heavy metals such as Pt and Pd that are close to the Stoner criterion may become magnetically polarized when interfaced with metallic FMs. This proximity-induced moment (PIM) in the NM layer is typically confined to the interface with the FM.^{68–74} In contrast, no PIM or a very small PIM has been measured in Pt layered with a range of oxide ferrimagnets.^{75–77} The origin of PIM is associated with hybridization across the interface.⁶⁸

In the spin-pumping model, the enhanced spin susceptibility in such proximity polarized NM materials has no role in the transmission of spin current across the interface as the Sharvin conductance is essentially unchanged.¹⁹ Furthermore, the non-equilibrium spin accumulation, μ_s , which drives the spin current, has no dependence on the Stoner enhancement through equilibrium polarization, even though the proximity spin density is affected. The tight binding model of interfacial enhancement of damping also does not explicitly consider PIM, with the enhancement in damping linked to SOC and d - d hybridization at the interface, although the latter is associated with the origin of PIM.

Although PIM is not explicitly represented in the original spin pumping model, the presence of PIM has been linked to quantitative values of key parameters, in particular, the spin mixing conductance and with PIM causing a de-phasing of the spin current that shortens the effective spin-diffusion length.^{78,79} Also, in relation to interfacial magnetism, enhanced spin-pumping, derived from damping observed in a FM layer coupled with another magnetic layer operating close to T_c , was explained in terms of enhancement of the interfacial spin conductance.^{80,81} Experimental studies of the influence of proximity polarization on damping and spin transport have generated conflicting results and interpretation, with experiments reporting that PIM has a no effect⁵¹ or a significant effect⁸² on damping and spin-pumping, or no effect at all on interfacial spin-transport.⁸³

To address this issue a recent comparative study measured PIM and the enhancement of damping in the same samples for two FM systems layered with Pt, in which a Au spacer layer of increasing thickness was introduced between the FM and Pt layers. Au was selected as it has a very small effect on damping and has a large spin-diffusion length. The relationship between the enhancement of damping and Pt PIM in these two FM systems is shown in Fig. 9. The results show a strong correlation between the enhancement of the damping and the magnitude of the Pt PIM, with the damping falling toward the bulk uncapped FM values when the Pt PIM is lost.⁷⁴ The two FM systems presented showed different structural behavior with the Pt PIM in CoFe/Au/Pt being closely associated with the FM/Pt interface, while in the NiFe/Au/Pt system, the Pt PIM extends further into the Pt layer due to some diffusion of the Ni into Au and Pt. The relationship between Pt PIM and damping was further evidenced in a system with a Cu

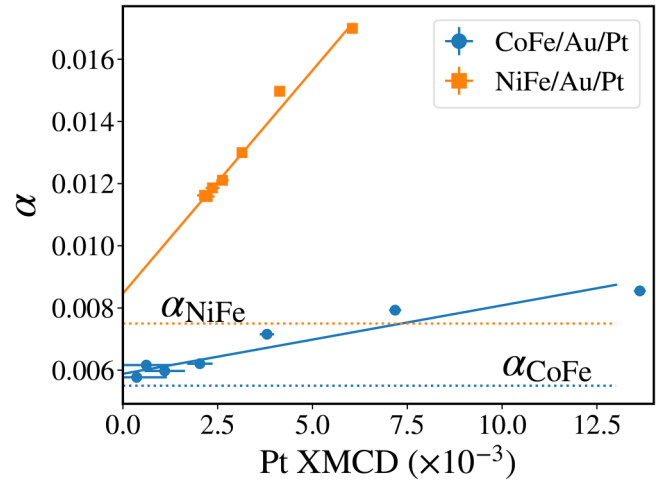


FIG. 9. Damping and Pt PIM signal from x-ray magnetic circular dichroism, XMCD, at the same Au spacer layer thicknesses for the CoFe (7 nm)/Au(t)/Pt (4 nm) and NiFe (7 nm)/Au(t)/Pt (4 nm) samples. The solid lines are linear fits. The dotted lines indicate the bulk damping for the ferromagnetic layers. Reproduced with the permission from Swindells *et al.*, Appl. Phys. Lett. **119**, 152401 (2021). Copyright 2021 AIP Publishing LLC.

spacer layer in the structure CoFe/Cu(t)/Pt, which showed the largest damping is associated with the highest Pt PIM and the lowest damping with the loss of Pt PIM.⁸⁴

V. DEVELOPMENTS IN RELATION TO SPIN TRANSPORT

A. Spin transport in multilayered systems

In addition to spin current created by precessing magnetization, the flow of charge current through a suitable NM layer can generate a significant orthogonal spin current that can propagate into a FM layer and exert a so-called spin-orbit torque on the magnetization.^{85,86} The implicit reciprocal nature of the spin current flow in spin-pumping and spin-transfer torques between FM and NM layers has been proven using Onsager's reciprocity relations, which showed that these are equivalent dynamic processes.⁸⁷ While the topical focus here is on enhanced damping in FM/NM systems, the relationship between spin-pumping and spin-transfer torque warrants an outline of the spin torque processes.

Amin and Stiles present a comprehensive description of spin transport including contributions from two such sources of torque.^{52,88} The first arises due to bulk SOC in a HM layer, which results in carriers with opposite spin polarization scattering in opposite directions. This is the spin Hall effect,^{89,90} in which a charge current generates a spin current that flows orthogonal to the charge current. A charge current flowing in-plane in a FM/HM bilayer produces an orthogonal spin current and an associated flow of spin angular momentum across the interface into the FM layer. This generates a torque described by $\vec{m} \times [\vec{m} \times (-\vec{x} \times \vec{z})] = \vec{m} \times [\vec{m} \times \vec{y}]$, where \vec{m} is the unit vector aligned with the magnetization, \vec{x} is the direction of the charge current, \vec{y} is the direction of spin current polarization, and \vec{z} is the direction of spin current propagation normal to

the interface. This torque is termed “damping-like” as it mathematically appears similar to the damping term in the LLG equation and causes the magnetization to drive toward a particular axis.

The second torque is attributed to the breaking of structural inversion symmetry in FM/HM systems.⁹¹ At the interface, an electric field shifts the Fermi surface in the FM material, resulting in a change to the majority and minority spin bands. This is termed the Rashba SOC. Without this SOC, there is no non-equilibrium spin density and hence no torque, likewise, if there is no exchange interaction between the magnetization and the local magnetization, no torque is generated.^{92,93} If the spin accumulation from the Rashba effect is not aligned with the magnetization, then a torque results of the form $\vec{m} \times (-\vec{x} \times \vec{z}) = \vec{m} \times \vec{y}$, which is referred to as a “field-like” torque because it acts to drive the magnetization to precess around a particular axis.⁸⁸

Amin and Stiles present a magnetoelectronic circuit theory including spin transport at interfaces with SOC that accounts for these torques.^{52,88} The inclusion of SOC to magnetoelectronic circuit theory is not trivial; interfacial SOC leads to the transfer of spin polarization to the lattice, which, in turn, affects the pumped current. This has been proposed as the source of many of the discrepancies between experimental results.^{57,94,95} Furthermore, additional spin-flip processes attributed to SOC, particularly, when the lattice at the interface acts as a sink for angular momentum, i.e., spin memory loss, were not accounted for in earlier magnetoelectronic circuit theory.

To account for SOC and in-plane electric fields, the spin and charge current densities are given by conductance tensor, G , defined using spin and charge indices in the 3D space and \vec{E} , the in-plane electric field. This allows for several key changes from conventional theory.⁵² First, this allows for the mathematical description of the flow of both in- and out-of-plane charge and spin currents. Second, the current densities depend on the values of the charge and spin accumulations rather than the difference, accounting for both non-zero averages of, and reductions in, charge and spin accumulations at the interface. Third, the conductivity tensor arising from interfacial spin-orbit scattering accounts for spin currents driven by an in-plane electric field.

For spin pumping, the conductance tensor introduced characterizes both spin memory loss and interface transparency. The interfacial transparency depends upon spin-orbit coupling, while spin memory loss was shown to depend on the interfacial exchange interaction. This interpretation resolves outstanding issues with experimental results, in particular, the claimed disagreement between the interfacial spin current and the actual spin current in Pt due to spin memory loss⁶⁶ and interface transparency.⁹⁵

B. The spin-diffusion length from spin pumping analysis

The spin-diffusion length, λ_{sd} , has been determined by a variety of methods, with values reported for specific metals varying over an order magnitude, for example, with values for both Pt and Pd ranging from 1 to more than 10 nm. λ_{sd} is explicit in the spin-pumping formalism and ferromagnetic resonance measurements have been used to determine λ_{sd} with this analysis. Such analysis typically produces low values for λ_{sd} compared to other methods.

Recent developments have sought to address this issue by considering the additional role of interface scattering and the thickness dependence of λ_{sd} in the NM layer.^{56,96–98} These require more extensive sample systems, measurements, and analysis than the single NM thickness analysis commonly reported.

As discussed earlier, there is good evidence that interfaces are responsible for additional scattering, which would contribute to the spin mixing conductance and reduce the apparent spin-diffusion length of the NM layer. Methods that effectively represent the spin dependent scattering at different interfaces allow for a consistent value of λ_{sd} to be obtained from spin-pumping analysis.⁹⁷ The inclusion of a thickness dependence of the spin-diffusion length into spin-pumping analysis is not so obvious. λ_{sd} is typically assumed to be a constant, but it is associated with electronic scattering processes and as such with the resistivity, ρ of the layer, which is thickness dependent. Taking the notion of the product $\lambda_{sd}\rho$ as a constant⁹⁹ and assuming an appropriate thickness dependence for ρ the bulk spin-diffusion length for Pt has been determined from spin-pumping analysis to be between 6.6 and 9.5 nm, which is significantly larger than the simpler constant λ_{sd} analysis that gives a value of 1.6 nm and closer to reports from other methods,^{100–102} although no interface scattering was specifically taken into account. Taking into account both interfacial scattering and the thickness dependence of λ_{sd} seems to improve the values for λ_{sd} obtained from spin-pumping analysis.

VI. SUMMARY AND CONCLUSIONS

The enhancement of ferromagnetic damping in FM/NM metallic systems has been widely studied experimentally over the past two decades. Theoretical explanations based on the electronic interactions across FM/NM interfaces have been developed using a tight binding model incorporating SOC and a spin transport model that invokes the pumping of spin current from the FM to NM layer. The spin-pumping concept has been widely taken up to analyze and explain a range of experimental observations.

The spin-pumping model has been successful in explaining the FM thickness dependence of the damping observed in FM/NM systems. While the role and thickness dependence of the NM layer in increasing the damping may be understood in terms of a combination of the enhancement of SOC and d - d hybridization at the interface and the pumping of spin current into the NM layer, which is governed by the spin-diffusion length of the NM metal and the spin-mixing conductance parameter that determines the flow of spin current into the NM.

Experiments controlling aspects of the interfaces have shown limitations in the early models and further developments in understanding have been made for the role of the interfacial region in the enhancement of damping, which includes details of the interface structure and a correlation of higher damping with larger PIM. The additional scattering attributed to the interface raises questions about the analysis of FM/NM systems in terms of the origin of the spin-mixing conductance and the derivation of the spin-diffusion length using the original spin-pumping analysis. More recent developments provide routes to overcome these limitations and obtain values for the spin-diffusion length closer to those obtained by other methods.

While open questions remain, currently, the enhancement of damping in FM/NM systems can be understood in terms, first of the direct electronic interactions at the interface between the FM and NM metals that locally enhances the SOC and leads to d - d hybridization and secondly by the absorption of spin current pumped into the NM layer by the electrochemical potential generated by the precessing FM. Spin-flip scattering determines the additional damping due to the absorption of this spin current, which occurs at both the interface and in the bulk of the NM layer due to the so-called spin memory loss at the interface and the spin-diffusion length of the NM metal, respectively. Details of the interfacial contributions to damping, such as the role of PIM, need further attention.

ACKNOWLEDGMENTS

The authors are grateful for funding from EPSRC for C.S. (No. 1771248), Ref. No. EP/P510476/1 and the Royal Society for D.A. (No. IF170030). The authors thank Aidan Hindmarch for critical reading and discussion that improved the manuscript.

AUTHOR DECLARATIONS

Conflict of Interest

The authors have no conflicts to disclose.

DATA AVAILABILITY

Data sharing is not applicable to this article as no new data were created or analyzed in this study.

REFERENCES

- ¹M. Bauer, J. Fassbender, B. Hillebrands, and R. Stamps, "Switching behavior of a stoner particle beyond the relaxation time limit," *Phys. Rev. B* **61**, 3410 (2000).
- ²N. L. Schryer and L. R. Walker, "The motion of 180° domain walls in uniform DC magnetic fields," *J. Appl. Phys.* **45**, 5406–5421 (1974).
- ³D. Atkinson, D. A. Allwood, C. C. Faulkner, G. Xiong, M. D. Cooke, and R. P. Cowburn, "Magnetic domain wall dynamics in a permalloy nanowire," *IEEE Trans. Magn.* **39**, 2663–2665 (2003).
- ⁴A. Mougín, M. Cormier, J. Adam, P. Metaxas, and J. Ferré, "Domain wall mobility, stability and walker breakdown in magnetic nanowires," *Europhys. Lett.* **78**, 57007 (2007).
- ⁵E. Lewis, D. Petit, L. O'Brien, A. Fernandez-Pacheco, J. Sampaio, A. Jausovec, H. Zeng, D. Read, and R. Cowburn, "Fast domain wall motion in magnetic comb structures," *Nat. Mater.* **9**, 980–983 (2010).
- ⁶D. M. Burn and D. Atkinson, "Suppression of walker breakdown in magnetic domain wall propagation through structural control of spin wave emission," *Appl. Phys. Lett.* **102**, 242414 (2013).
- ⁷M. A. Schoen, D. Thonig, M. L. Schneider, T. Silva, H. T. Nembach, O. Eriksson, O. Karis, and J. M. Shaw, "Ultra-low magnetic damping of a metallic ferromagnet," *Nat. Phys.* **12**, 839–842 (2016).
- ⁸R. Silsbee, A. Janossy, and P. Monod, "Coupling between ferromagnetic and conduction-spin-resonance modes at a ferromagnetic-normal-metal interface," *Phys. Rev. B* **19**, 4382 (1979).
- ⁹B. Heinrich, K. Urquhart, A. Arrott, J. Cochran, K. Myrtle, and S. Purcell, "Ferromagnetic-resonance study of ultrathin bcc Fe (100) films grown epitaxially on fcc Ag (100) substrates," *Phys. Rev. Lett.* **59**, 1756 (1987).
- ¹⁰S. Mizukami, Y. Ando, and T. Miyazaki, "The study on ferromagnetic resonance linewidth for NM/80NiFe/NM (nm = Cu, Ta, Pd and Pt) films," *Jpn. J. Appl. Phys.* **40**, 580 (2001).
- ¹¹S. Mizukami, Y. Ando, and T. Miyazaki, "Ferromagnetic resonance linewidth for NM/80NiFe/NM films (NM = Cu, Ta, Pd and Pt)," *J. Magn. Magn. Mater.* **226–230**, 1640–1642 (2001).
- ¹²R. Urban, G. Woltersdorf, and B. Heinrich, "Gilbert damping in single and multilayer ultrathin films: Role of interfaces in nonlocal spin dynamics," *Phys. Rev. Lett.* **87**, 217204 (2001).
- ¹³S. Mizukami, Y. Ando, and T. Miyazaki, "Effect of spin diffusion on gilbert damping for a very thin permalloy layer in Cu/permalloy/Cu/Pt films," *Phys. Rev. B* **66**, 104413 (2002).
- ¹⁴E. Saitoh, M. Ueda, H. Miyajima, and G. Tatara, "Conversion of spin current into charge current at room temperature: Inverse spin-Hall effect," *Appl. Phys. Lett.* **88**, 182509 (2006).
- ¹⁵L. Berger, "Emission of spin waves by a magnetic multilayer traversed by a current," *Phys. Rev. B* **54**, 9353 (1996).
- ¹⁶L. Berger, "Effect of interfaces on gilbert damping and ferromagnetic resonance linewidth in magnetic multilayers," *J. Appl. Phys.* **90**, 4632–4638 (2001).
- ¹⁷Y. Tserkovnyak, A. Brataas, and G. E. Bauer, "Enhanced gilbert damping in thin ferromagnetic films," *Phys. Rev. Lett.* **88**, 117601 (2002).
- ¹⁸Y. Tserkovnyak, A. Brataas, and G. E. Bauer, "Spin pumping and magnetization dynamics in metallic multilayers," *Phys. Rev. B* **66**, 224403 (2002).
- ¹⁹Y. Tserkovnyak, A. Brataas, G. E. Bauer, and B. I. Halperin, "Nonlocal magnetization dynamics in ferromagnetic heterostructures," *Rev. Mod. Phys.* **77**, 1375 (2005).
- ²⁰E. Simánek and B. Heinrich, "Gilbert damping in magnetic multilayers," *Phys. Rev. B* **67**, 144418 (2003).
- ²¹E. Barati, M. Cinal, D. Edwards, and A. Umerski, "Gilbert damping in magnetic layered systems," *Phys. Rev. B* **90**, 014420 (2014).
- ²²L. Landau and L. EM, "On the theory of the dispersion of magnetic permeability in ferromagnetic bodies," *Perspectives in Theoretical Physics* (Elsevier, 1992), pp 51–65.
- ²³T. L. Gilbert, "A Lagrangian formulation of the gyromagnetic equation of the magnetization field," *Phys. Rev.* **100**, 1243 (1955).
- ²⁴C. Kittel, "On the theory of ferromagnetic resonance absorption," *Phys. Rev.* **73**, 155 (1948).
- ²⁵Y. Wei, "Ferromagnetic resonance as a probe of magnetization dynamics: A study of FeCo thin films and trilayers," Ph.D. thesis (Acta Universitatis Upsaliensis, 2015).
- ²⁶E. Olsen, *Applied Magnetism: A Study in Quantities* (Centrex, 1966).
- ²⁷K. Baberschke, "Ferromagnetic resonance in nanostructures, rediscovering its roots in paramagnetic resonance," *J. Phys. Conf. Ser.* **324**, 012011 (2011).
- ²⁸R. Rowan-Robinson, A. Hindmarch, and D. Atkinson, "Enhanced electron-magnon scattering in ferromagnetic thin films and the breakdown of the Mott two-current model," *Phys. Rev. B* **90**, 104401 (2014).
- ²⁹O. Chubykalo-Fesenko, U. Nowak, R. W. Chantrell, and D. Garanin, "Dynamic approach for micromagnetics close to the Curie temperature," *Phys. Rev. B* **74**, 094436 (2006).
- ³⁰A. Lyberatos, D. V. Berkov, and R. W. Chantrell, "A method for the numerical simulation of the thermal magnetization fluctuations in micromagnetics," *J. Phys.: Condens. Matter* **5**, 8911 (1993).
- ³¹B. Heinrich, J. Cochran, and R. Hasegawa, "FMR linebroadening in metals due to two-magnon scattering," *J. Appl. Phys.* **57**, 3690–3692 (1985).
- ³²Y. Wei, S. L. Chin, and P. Svedlindh, "On the frequency and field linewidth conversion of ferromagnetic resonance spectra," *J. Phys. D* **48**, 335005 (2015).
- ³³V. Kamberský, "On the Landau–Lifshitz relaxation in ferromagnetic metals," *Can. J. Phys.* **48**, 2906–2911 (1970).
- ³⁴V. Kamberský, "On ferromagnetic resonance damping in metals," *Czech. J. Phys. B* **26**, 1366–1383 (1976).
- ³⁵K. Gilmore, Y. U. Idzerda, and M. D. Stiles, "Spin-orbit precession damping in transition metal ferromagnets," *J. Appl. Phys.* **103**, 07D303 (2008).
- ³⁶K. Gilmore, Y. Idzerda, and M. D. Stiles, "Identification of the dominant precession-damping mechanism in Fe, Co, and Ni by first-principles calculations," *Phys. Rev. Lett.* **99**, 027204 (2007).

- ³⁷S. Azzawi, A. Hindmarch, and D. Atkinson, "Magnetic damping phenomena in ferromagnetic thin-films and multilayers," *J. Phys. D* **50**, 473001 (2017).
- ³⁸R. Elliott, "Spin-orbit coupling in band theory—character tables for some 'double' space groups," *Phys. Rev.* **96**, 280 (1954).
- ³⁹Y. Yafet, "g Factors and spin-lattice relaxation of conduction electrons," *Solid State Phys.* **14**, 1–98 (1963).
- ⁴⁰L. Szolnoki, B. Dóra, A. Kiss, J. Fabian, and F. Simon, "Intuitive approach to the unified theory of spin relaxation," *Phys. Rev. B* **96**, 245123 (2017).
- ⁴¹M. I. Dyakonov and V. I. Perel, "Spin relaxation of conduction electrons in non-centrosymmetric semiconductors," *Sov. Phys. Solid State* **13**, 3023–3026 (1972).
- ⁴²R. Freeman, A. Zholud, Z. Dun, H. Zhou, and S. Urazhdin, "Evidence for Dyakonov-Perel-like spin relaxation in Pt," *Phys. Rev. Lett.* **120**, 067204 (2018).
- ⁴³Y. Otani and T. Kimura, "Manipulation of spin currents in metallic systems," *Philos. Trans. R. Soc. A* **369**, 3136–3149 (2011).
- ⁴⁴J. Bass and W. P. Pratt Jr, "Spin-diffusion lengths in metals and alloys, and spin-flipping at metal/metal interfaces: An experimentalist's critical review," *J. Phys.: Condens. Matter* **19**, 183201 (2007).
- ⁴⁵J. Kunes and V. Kambarský, "First-principles investigation of the damping of fast magnetization precession in ferromagnetic 3D metals," *Phys. Rev. B* **65**, 212411 (2002).
- ⁴⁶L. Berger, "Precession of conduction-electron spins near an interface between normal and magnetic metals," *IEEE Trans. Magn.* **31**, 3871–3873 (1995).
- ⁴⁷A. Brataas, Y. Tserkovnyak, G. E. Bauer, and B. I. Halperin, "Spin battery operated by ferromagnetic resonance," *Phys. Rev. B* **66**, 060404 (2002).
- ⁴⁸A. Brataas, Y. Tserkovnyak, and G. E. Bauer, "Scattering theory of Gilbert damping," *Phys. Rev. Lett.* **101**, 037207 (2008).
- ⁴⁹K. Ando, "Dynamical generation of spin currents," *Semicond. Sci. Technol.* **29**, 043002 (2014).
- ⁵⁰P. Brouwer, "Scattering approach to parametric pumping," *Phys. Rev. B* **58**, R10135 (1998).
- ⁵¹M. Weiler, M. Althammer, M. Schreier, J. Lotze, M. Pernpeintner, S. Meyer, H. Huebl, R. Gross, A. Kamra, J. Xiao, Y. Chen, H. Jiao, G. Bauer, and S. Goennenwein, *Phys. Rev. Lett.* **111**, 176601 (2013).
- ⁵²V. P. Amin and M. D. Stiles, "Spin transport at interfaces with spin-orbit coupling: Formalism," *Phys. Rev. B* **94**, 104419 (2016).
- ⁵³X. Jia, Y. Li, K. Xia, and G. E. Bauer, "Angular momentum transfer torques in spin valves with perpendicular magnetization," *Phys. Rev. B* **84**, 134403 (2011).
- ⁵⁴X. Jia, K. Liu, K. Xia, and G. E. Bauer, "Spin transfer torque on magnetic insulators," *Europhys. Lett.* **96**, 17005 (2011).
- ⁵⁵M. Costache, S. Watts, C. Van Der Wal, and B. Van Wees, "Electrical detection of spin pumping: DC voltage generated by ferromagnetic resonance at ferromagnet/nonmagnet contact," *Phys. Rev. B* **78**, 064423 (2008).
- ⁵⁶C. Swindells, A. Hindmarch, A. Gallant, and D. Atkinson, "Spin transport across the interface in ferromagnetic/nonmagnetic systems," *Phys. Rev. B* **99**, 064406 (2019).
- ⁵⁷Y. Liu, Z. Yuan, R. J. Wesselink, A. A. Starikov, and P. J. Kelly, "Interface enhancement of Gilbert damping from first principles," *Phys. Rev. Lett.* **113**, 207202 (2014).
- ⁵⁸M. Belmeguenai, M. Gabor, F. Zighem, N. Challab, T. Petrisor, R. Mos, and C. Tiusan, *J. Phys. D: Appl. Phys.* **51**, 045002 (2018).
- ⁵⁹L. Zhu, D. C. Ralph, and R. A. Buhrman, "Effective spin-mixing conductance of heavy-metal-ferromagnet interfaces," *Phys. Rev. Lett.* **123**, 057203 (2019).
- ⁶⁰S. Azzawi, A. Ganguly, M. Tokac, R. Rowan-Robinson, J. Sinha, A. Hindmarch, A. Barman, and D. Atkinson, "Evolution of damping in ferromagnetic/nonmagnetic thin film bilayers as a function of nonmagnetic layer thickness," *Phys. Rev. B* **93**, 054402 (2016).
- ⁶¹J. King, A. Ganguly, D. Burn, S. Pal, E. Sallabank, T. Hase, A. Hindmarch, A. Barman, and D. Atkinson, "Local control of magnetic damping in ferromagnetic/non-magnetic bilayers by interfacial intermixing induced by focused ion-beam irradiation," *Appl. Phys. Lett.* **104**, 242410 (2014).
- ⁶²A. Ganguly, S. Azzawi, S. Saha, J. King, R. Rowan-Robinson, A. Hindmarch, J. Sinha, D. Atkinson, and A. Barman, "Tunable magnetization dynamics in interfacially modified Ni₈₁Fe₁₉/Pt bilayer thin film microstructures," *Sci. Rep.* **5**, 17596 (2015).
- ⁶³M. Tokac, S. Bunyavev, G. Kakazei, D. Schmool, D. Atkinson, and A. Hindmarch, "Interfacial structure dependent spin mixing conductance in cobalt thin films," *Phys. Rev. Lett.* **115**, 056601 (2015).
- ⁶⁴A. Cahaya, A. Leon, and G. Bauer, *Phys. Rev. B* **96**, 144434 (2017).
- ⁶⁵H. Kurt, R. Loloee, K. Eid, W. Pratt, and J. Bass, *Appl. Phys. Lett.* **81**, 4787 (2002).
- ⁶⁶J. Rojas-Sánchez, N. Reyren, P. Laczkowski, W. Savero, J. Attané, C. Deranlot, M. Jamet, J. George, L. Vila, and H. Jaffrès, *Phys. Rev. Lett.* **112**, 106602 (2014).
- ⁶⁷K. Chen and S. Zhang, "Spin pumping in the presence of spin-orbit coupling," *Phys. Rev. Lett.* **114**, 126602 (2015).
- ⁶⁸F. Wilhelm, P. Pouloupoulos, G. Ceballos, H. Wende, K. Baberschke, P. Srivastava, D. Benea, H. Ebert, M. Angelakeris, N. Flevaris *et al.*, "Layer-resolved magnetic moments in Ni/Pt multilayers," *Phys. Rev. Lett.* **85**, 413 (2000).
- ⁶⁹F. Wilhelm, P. Pouloupoulos, H. Wende, A. Scherz, K. Baberschke, M. Angelakeris, N. K. Flevaris, and A. Rogalev, "Systematics of the induced magnetic moments in 5D layers and the violation of the third Hund's rule," *Phys. Rev. Lett.* **87**, 207202 (2001).
- ⁷⁰F. Wilhelm, M. Angelakeris, N. Jaouen, P. Pouloupoulos, E. T. Papaioannou, C. Mueller, P. Fumagalli, A. Rogalev, and N. K. Flevaris, "Magnetic moment of Au at Au/Co interfaces: A direct experimental determination," *Phys. Rev. B* **69**, 220404 (2004).
- ⁷¹R. Rowan-Robinson, A. Stashkevich, Y. Roussigné, M. Belmeguenai, S. Chérif, A. Thiaville, T. Hase, A. Hindmarch, and D. Atkinson, *Sci. Rep.* **7**, 16835 (2017).
- ⁷²O. Inyang, L. Bouchenoire, B. Nicholson, M. Tokac, R. Rowan-Robinson, C. Kinane, and A. Hindmarch, "Threshold interface magnetization required to induce magnetic proximity effect," *Phys. Rev. B* **100**, 174418 (2019).
- ⁷³C. Swindells, B. Nicholson, O. Inyang, Y. Choi, T. Hase, and D. Atkinson, "Proximity-induced magnetism in Pt layered with rare-earth-transition-metal ferrimagnetic alloys," *Phys. Rev. Res.* **2**, 033280 (2020).
- ⁷⁴C. Swindells, H. Głowiński, Y. Choi, D. Haskel, P. Michałowski, T. Hase, P. Kuświk, and D. Atkinson, "Proximity-induced magnetism and the enhancement of damping in ferromagnetic/heavy metal systems," *Appl. Phys. Lett.* **119**, 152401 (2021).
- ⁷⁵H. Wu, Q. Zhang, C. Wan, S. S. Ali, Z. Yuan, L. You, J. Wang, Y. Choi, and X. Han, "Spin Hall magnetoresistance in CoFe₂O₄/Pt films," *IEEE Trans. Magn.* **51**, 1–4 (2015).
- ⁷⁶M. Collet, R. Mattana, J.-B. Moussy, K. Ollefs, S. Collin, C. Deranlot, A. Anane, V. Cros, F. Petroff, F. Wilhelm *et al.*, "Investigating magnetic proximity effects at ferrite/Pt interfaces," *Appl. Phys. Lett.* **111**, 202401 (2017).
- ⁷⁷M. Valvidares, N. Dix, M. Isasa, K. Ollefs, F. Wilhelm, A. Rogalev, F. Sánchez, E. Pellegrin, A. Bedoya-Pinto, P. Gargiani *et al.*, "Absence of magnetic proximity effects in magnetoresistive Pt/CoFe₂O₄ hybrid interfaces," *Phys. Rev. B* **93**, 214415 (2016).
- ⁷⁸J. Foros, G. Woltersdorf, B. Heinrich, and A. Brataas, "Scattering of spin current injected in Pd (001)," *J. Appl. Phys.* **97**, 10A714 (2005).
- ⁷⁹P. Omelchenko, E. Girt, and B. Heinrich, "Test of spin pumping into proximity-polarized Pt by in-phase and out-of-phase pumping in Py/Pt/Py," *Phys. Rev. B* **100**, 144418 (2019).
- ⁸⁰Y. Ohnuma, H. Adachi, E. Saitoh, and S. Maekawa, "Enhanced DC spin pumping into a fluctuating ferromagnet near TC," *Phys. Rev. B* **89**, 174417 (2014).
- ⁸¹R. Bansal, N. Chowdhury, and P. Muduli, "Proximity effect induced enhanced spin pumping in Py/Gd at room temperature," *Appl. Phys. Lett.* **112**, 262403 (2018).
- ⁸²M. Caminala, A. Ghosh, S. Auffret, U. Ebels, K. Ollefs, F. Wilhelm, A. Rogalev, and W. Bailey, "Spin pumping damping and magnetic proximity effect in Pd and Pt spin-sink layers," *Phys. Rev. B* **94**, 014414 (2016).
- ⁸³L. Zhu, D. Ralph, and R. Buhrman, "Irrelevance of magnetic proximity effect to spin-orbit torques in heavy-metal/ferromagnet bilayers," *Phys. Rev. B* **98**, 134406 (2018).
- ⁸⁴C. Swindells, H. Głowiński, Y. Choi, D. Haskel, P. Michałowski, T. Hase, F. Stobiecki, P. Kuświk, and D. Atkinson, "Magnetic damping in ferromagnetic/heavy-metal systems: The role of interfaces and the relation to proximity-induced magnetism," *Phys. Rev. B* **105**, 094433 (2022).

- ⁸⁵K. Ando, S. Takahashi, K. Harii, K. Sasage, J. Ieda, S. Maekawa, and E. Saitoh, "Electric manipulation of spin relaxation using the spin Hall effect," *Phys. Rev. Lett.* **101**, 036601 (2008).
- ⁸⁶L. Liu, O. Lee, T. Gudmundsen, D. Ralph, and R. Buhrman, "Current-induced switching of perpendicularly magnetized magnetic layers using spin torque from the spin Hall effect," *Phys. Rev. Lett.* **109**, 096602 (2012).
- ⁸⁷A. Brataas, Y. Tserkovnyak, G. Bauer, and P. J. Kelly, "Spin pumping and spin transfer," *Spin Curr.* **17**, 87–135 (2012).
- ⁸⁸V. Amin and M. Stiles, "Spin transport at interfaces with spin-orbit coupling: Phenomenology," *Phys. Rev. B* **94**, 104420 (2016).
- ⁸⁹J. Hirsch, "Spin Hall effect," *Phys. Rev. Lett.* **83**, 1834 (1999).
- ⁹⁰A. Hoffmann, "Spin Hall effects in metals," *IEEE Trans. Magn.* **49**, 5172–5193 (2013).
- ⁹¹I. M. Miron, K. Garello, G. Gaudin, P.-J. Zermatten, M. V. Costache, S. Auffret, S. Bandiera, B. Rodmacq, A. Schuhl, and P. Gambardella, "Perpendicular switching of a single ferromagnetic layer induced by in-plane current injection," *Nature* **476**, 189–193 (2011).
- ⁹²A. Manchon and S. Zhang, "Theory of spin torque due to spin-orbit coupling," *Phys. Rev. B* **79**, 094422 (2009).
- ⁹³H. B. M. Saidaoui and A. Manchon, "Spin-swapping transport and torques in ultrathin magnetic bilayers," *Phys. Rev. Lett.* **117**, 036601 (2016).
- ⁹⁴M. Obstbaum, M. Härtinger, H. Bauer, T. Meier, F. Swientek, C. Back, and G. Woltersdorf, "Inverse spin Hall effect in $\text{Ni}_{81}\text{Fe}_{19}$ /normal-metal bilayers," *Phys. Rev. B* **89**, 060407 (2014).
- ⁹⁵W. Zhang, W. Han, X. Jiang, S.-H. Yang, and S. S. Parkin, "Role of transparency of platinum-ferromagnet interfaces in determining the intrinsic magnitude of the spin Hall effect," *Nat. Phys.* **11**, 496–502 (2015).
- ⁹⁶A. Kumar, S. Akansel, H. Stopfel, M. Fazlali, J. Åkerman, R. Brucas, and P. Svedlindh, "Spin transfer torque ferromagnetic resonance induced spin pumping in the Fe/Pd bilayer system," *Phys. Rev. B* **95**, 064406 (2017).
- ⁹⁷X. Tao, Q. Liu, B. Miao, R. Yu, Z. Feng, L. Sun, B. You, J. Du, K. Chen, S. Zhang *et al.*, "Self-consistent determination of spin Hall angle and spin diffusion length in Pt and Pd: The role of the interface spin loss," *Sci. Adv.* **4**, eaat1670 (2018).
- ⁹⁸K. Roy, "Estimating the spin diffusion length and the spin Hall angle from spin pumping induced inverse spin Hall voltages," *Phys. Rev. B* **96**, 174432 (2017).
- ⁹⁹M.-H. Nguyen, D. Ralph, and R. Buhrman, *Phys. Rev. Lett.* **116**, 126601 (2016).
- ¹⁰⁰O. Mosendz, J. Pearson, F. Fradin, G. Bauer, S. Bader, and A. Hoffmann, *Phys. Rev. Lett.* **104**, 046601 (2010).
- ¹⁰¹Y. Niimi, D. Wei, H. Idzuchi, T. Wakamura, T. Kato, and Y. Otani, *Phys. Rev. Lett.* **110**, 016805 (2013).
- ¹⁰²H. Nguyen, W. Pratt, and J. Bass, *J. Magn. Magn. Mater.* **361**, 30 (2014).